

NNLO HTLpt predictions for the curvature of the QCD phase transition line

Michael Strickland

Kent State University
Kent, OH USA

N. Haque and MS, Phys. Rev. C 103, 031901 (2021) [arXiv:2011.06938]

N. Haque, A. Bandyopadhyay, J.O. Andersen, M.G. Mustafa, MS, and N. Su, JHEP 2014, 5, 1-46 (2014) [arXiv:1402.6907]

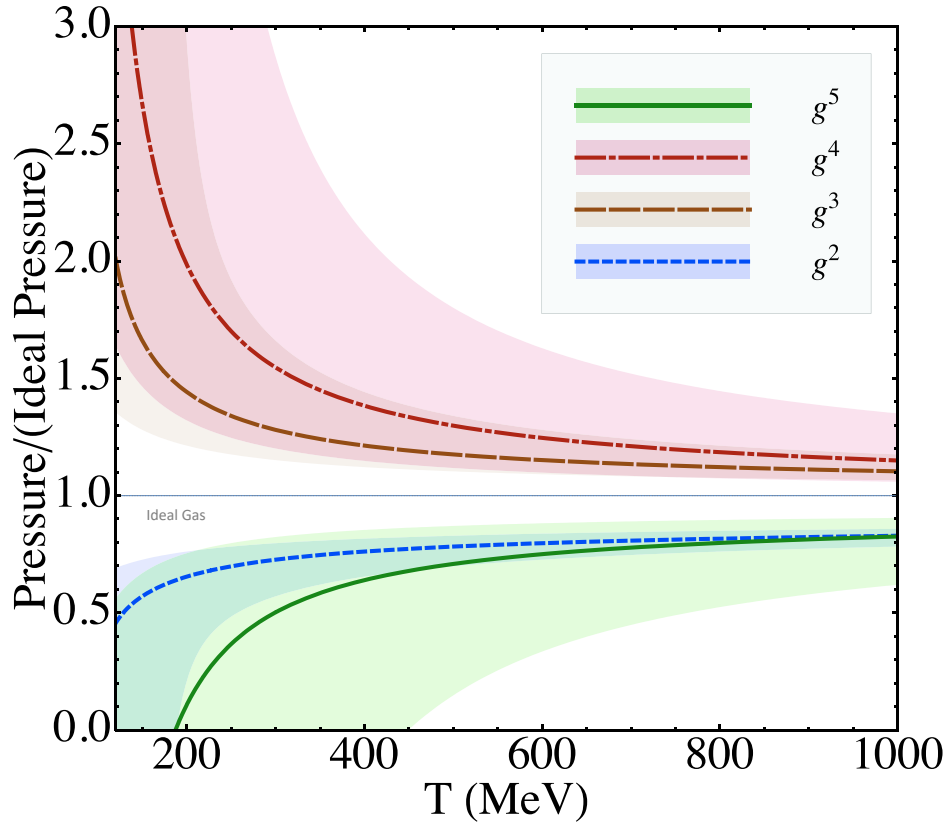
Confinement XV, Stavanger, Norway
August 1, 2022



U.S. DEPARTMENT OF
ENERGY

Naïve pQCD thermodynamics

- QCD free energy at finite T known up to three loops (g^5) since 1994
(Shuryak & Chin, Kapusta, Toimela, Arnold, Zhai, Kastening, Braaten, Nieto)
- Coefficient at $O(g^6 \log g)$ also known
(Kajantie, Laine, Rummukainen, Schröder)
- Extension to finite chemical potential
(Vuorinen)
- Need temperatures on the order of $T \sim 10^5$ GeV for convergence
- Similar problem in QED and scalar theories → the problem is not specific to QCD
- **Bad convergence is related to improper treatment of soft momenta**



Simple Case – Anharmonic Oscillator

- Consider quantum mechanics in an anharmonic potential

$$V(x) = \frac{1}{2}\omega^2 x^2 + \frac{g}{4}x^4 \quad (\omega^2, g > 0)$$

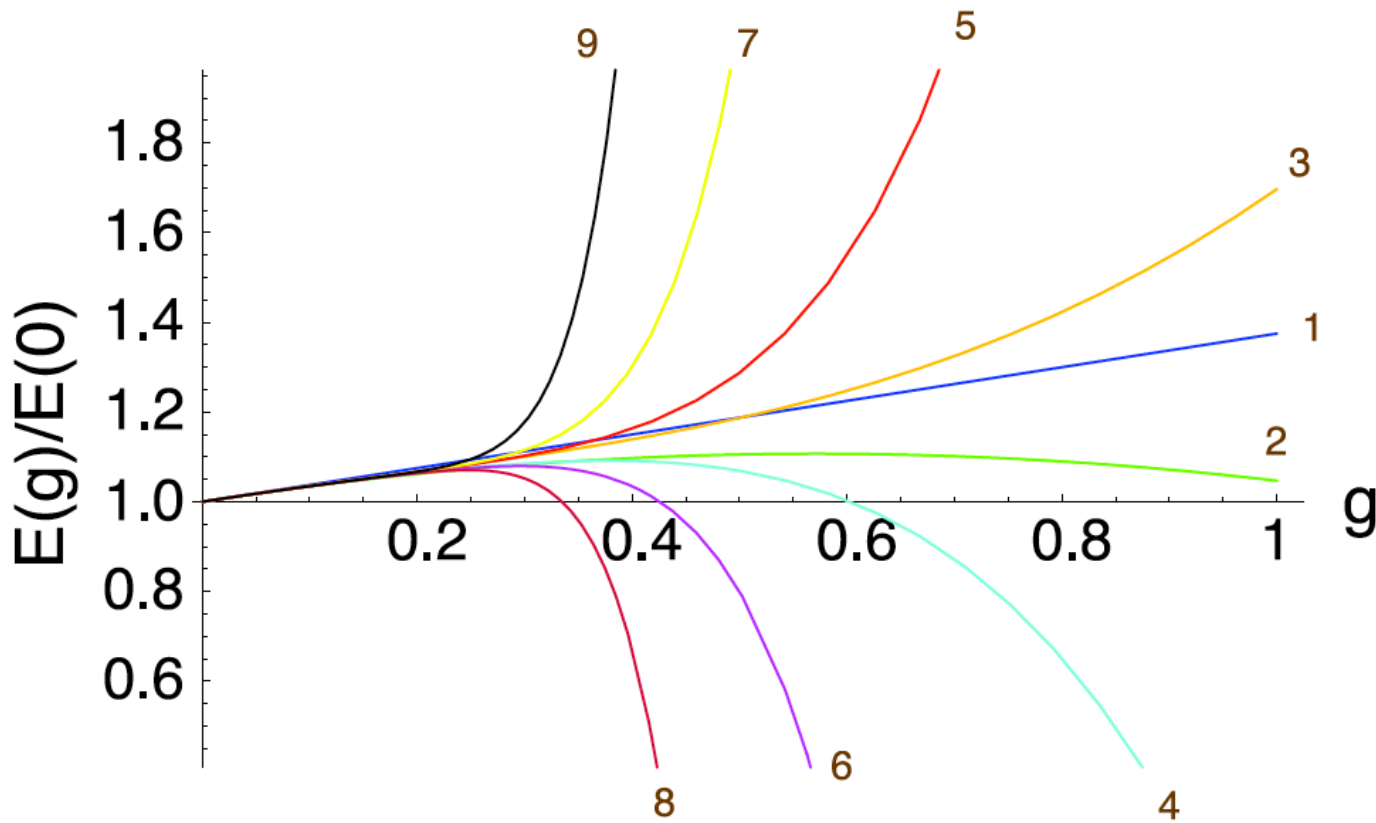
- Weak-coupling expansion of the ground state energy is known up to all orders
(Bender and Wu 69/73)

$$E(g) = \omega \sum_{n=0}^{\infty} c_n^{\text{BW}} \left(\frac{g}{4\omega^3} \right)^n, \quad c_n^{\text{BW}} = \left\{ \frac{1}{2}, \frac{3}{4}, -\frac{21}{8}, \frac{333}{16}, -\frac{30885}{16}, \dots \right\}$$

$$\lim_{n \rightarrow \infty} c_n^{\text{BW}} = (-1)^{n+1} \sqrt{\frac{6}{\pi^3}} 3^n (n - \frac{1}{2})!$$

- Factorial growth → expansion is an asymptotic series with zero radius of convergence!

Asymptotic Series



Variational Perturbation Theory

- Split the harmonic term into two pieces and treat the second as part of the interaction
(Janke and Kleinert 95)

$$\omega^2 \rightarrow \Omega^2 + (\omega^2 - \Omega^2) \implies E_N(g, r) = \Omega \sum_{n=0}^N c_n(r) \left(\frac{g}{4\Omega^3} \right)^n \quad r \equiv \frac{2}{g} (\omega^2 - \Omega^2)$$

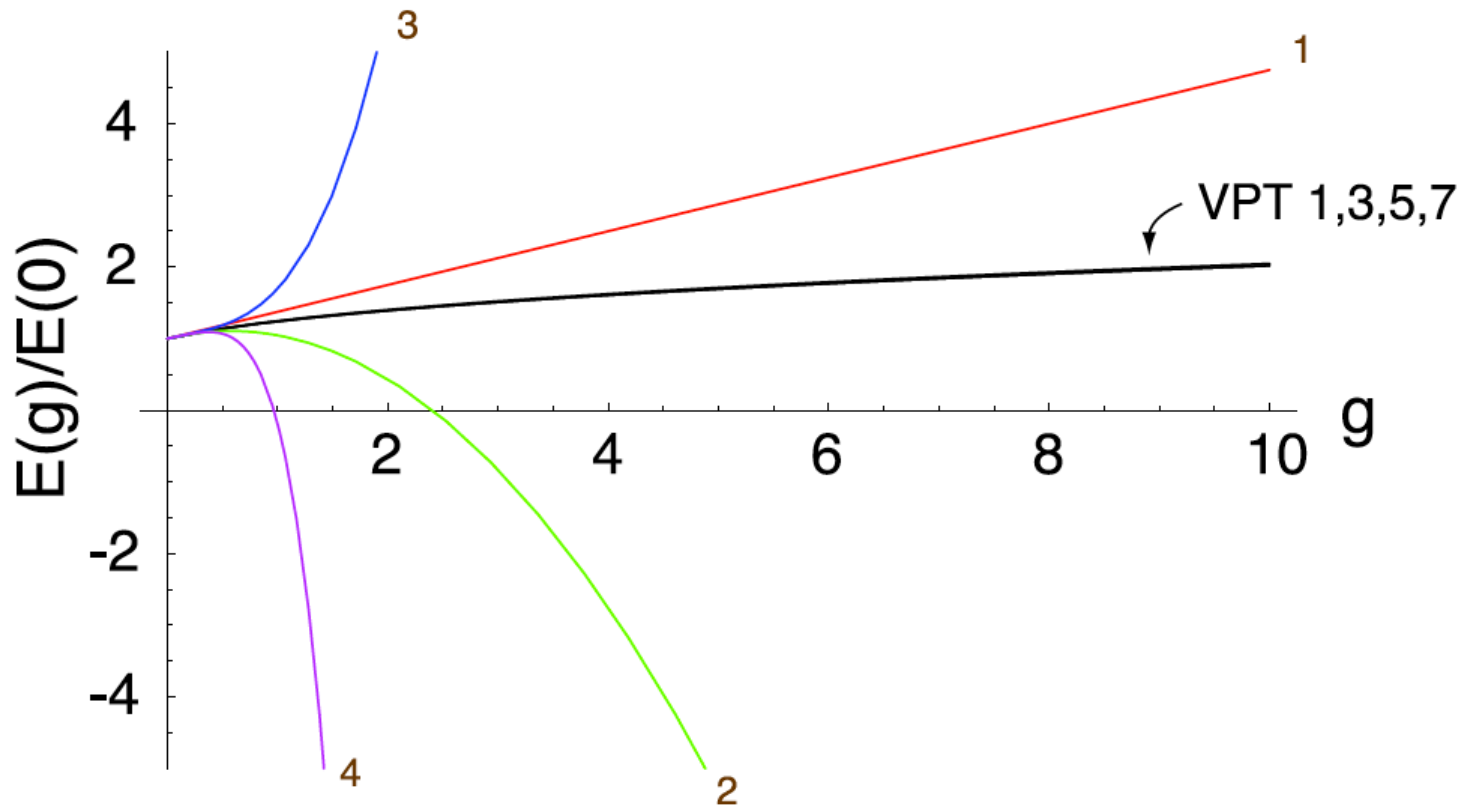
- The coefficients c_n can be computed analytically in this case

$$c_n(r) = \sum_{j=0}^n c_j^{\text{BW}} \binom{(1-3j)/2}{n-j} (2r\Omega)^{n-j}$$

- Fix Ω by imposing variational condition that ground state energy is minimized

$$\frac{\partial E_N}{\partial \Omega} \Big|_{\Omega=\Omega_N} = 0 \quad \rightarrow \text{"Gap equation"}$$

Variational Perturbation Theory



Hard Thermal Loops (HTLs)

In a high temperature QGP one must “resum” a certain class of diagrams which have hard internal (loop) momentum $p_{\text{hard}} \sim T$ and soft external momentum $p_{\text{soft}} \sim gT$

$$\Pi \approx \left(\text{Diagram 1} + \text{Diagram 2} + \text{Diagram 3} \right) g^2 T^2$$

At finite temperature, there are transverse **and** longitudinal gluons

$$\Pi_T(\omega, p) = \frac{m_D^2}{2} \frac{\omega^2}{p^2} \left[1 + \frac{p^2 - \omega^2}{2\omega p} \log \frac{\omega + p}{\omega - p} \right]$$

$$\Pi_L(\omega, p) = m_D^2 \left[1 - \frac{\omega}{2p} \log \frac{\omega + p}{\omega - p} \right]$$

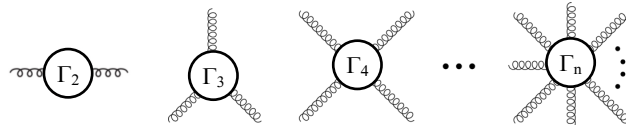
Gluons \rightarrow quasiparticles with a temperature dependent mass which is proportional to the temperature. At leading order one has

$$\lim_{\omega \rightarrow 0} \Pi_T(\omega, p) = 0$$

$$\lim_{\omega \rightarrow 0} \Pi_L(\omega, p) = m_D^2$$

$$m_D^2 = \frac{1}{3} \left(N_c + \frac{1}{2} N_f \right) g^2 T^2$$

$$\mathcal{L}_{\text{HTL}} = -\frac{1}{2} m_D^2 \text{Tr} \left(G_{\mu\alpha} \left\langle \frac{y^\alpha y^\beta}{(y \cdot D)^2} \right\rangle_y G^\mu_\beta \right) + i m_q^2 \bar{\psi} \gamma^\mu \left\langle \frac{y^\mu}{y \cdot D} \right\rangle_y \psi,$$



Silin, V., Sov. Phys. JETP 11, 1136 (1960)
 Kalashnikov, O. K., and V. V. Klimov, Sov. J. Nucl. Phys. 31, 699 (1980)
 Weldon, H. A., Phys. Rev. D26, 1394, (1982)
 Braaten, E., and R. D. Pisarski, Phys. Rev. D45, 1827 (1992)

[Andersen, Braaten, and MS, 99 → 02]

HTLpt Action

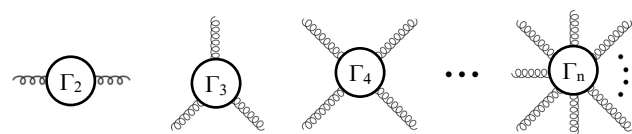
- Can express an infinite number of HTL-dressed n-point functions concisely in terms of an HTL effective action, \mathcal{L}_{HTL}
- Expanding \mathcal{L}_{HTL} to quadratic order in A gives dressed propagator (2-point function)
- Expanding to cubic order in A gives the dressed gluon three-vertex
- Expanding to quartic order in A gives dressed gluon four-vertex
- And so on . . . contains an infinite number of higher order vertices which all exactly satisfy the appropriate Slavnov-Taylor identities

$$\mathcal{L} = (\mathcal{L}_{\text{QCD}} + \mathcal{L}_{\text{HTL}}) \Big|_{g_s \rightarrow \sqrt{\delta} g_s} + \Delta \mathcal{L}_{\text{HTL}}$$

[Andersen, Braaten, and MS, 99 → 02]

$$\begin{aligned} \mathcal{L}_{\text{QCD}} = & -\frac{1}{2} \text{Tr} [G_{\mu\nu} G^{\mu\nu}] + i\bar{\psi}\gamma^\mu D_\mu \psi \\ & + \mathcal{L}_{\text{gf}} + \mathcal{L}_{\text{gh}} + \Delta \mathcal{L}_{\text{QCD}} \end{aligned}$$

$$\begin{aligned} \mathcal{L}_{\text{HTL}} = & -\frac{1}{2}(1-\delta)m_D^2 \text{Tr} \left(G_{\mu\alpha} \left\langle \frac{y^\alpha y^\beta}{(y \cdot D)^2} \right\rangle_y G^\mu{}_\beta \right) \\ & +(1-\delta)im_q^2 \bar{\psi}\gamma^\mu \left\langle \frac{y_\mu}{y \cdot D} \right\rangle_y \psi, \end{aligned}$$



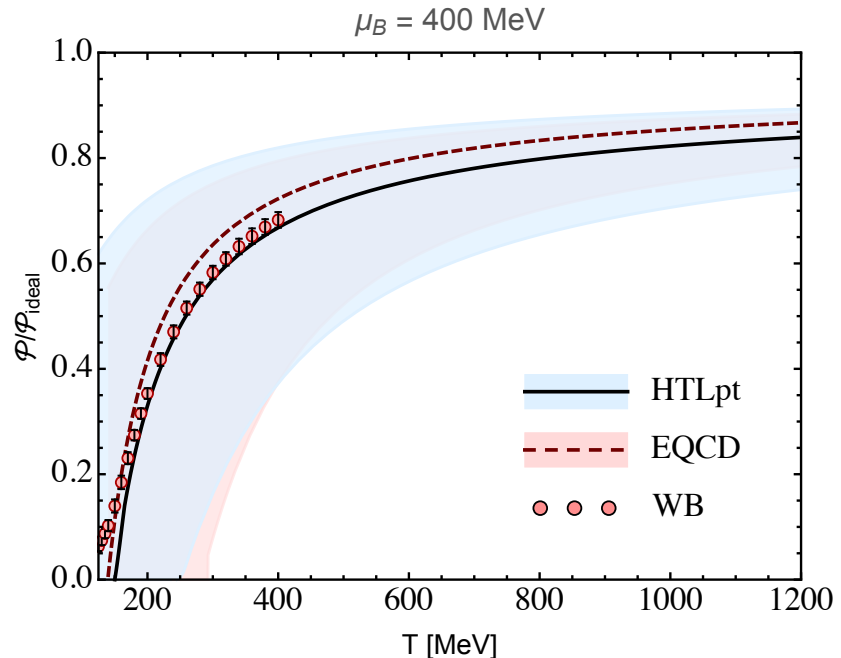
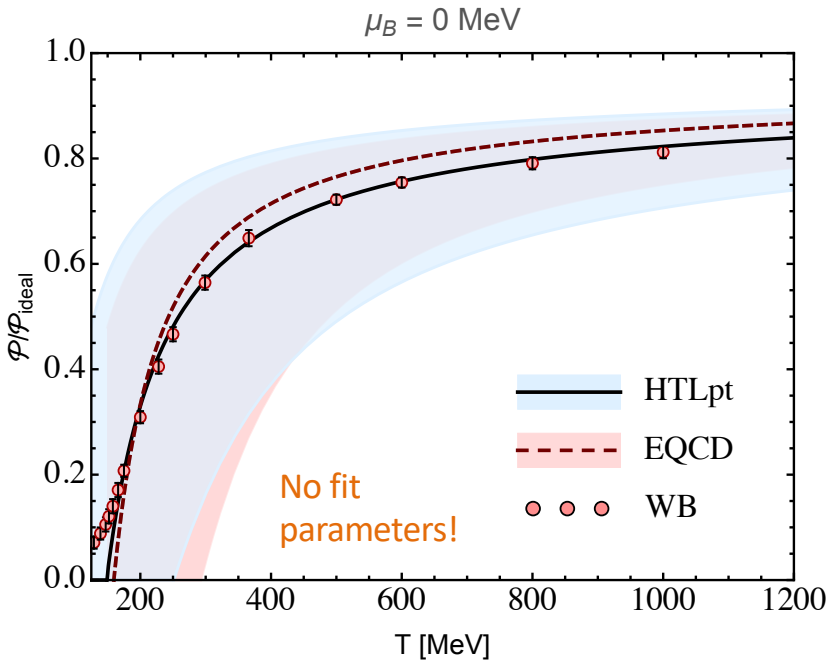
NNLO Hard Thermal Loop Perturbation Theory (HTLpt)

- HTLpt reorganization improves the convergence of perturbation theory compared to strict perturbation theory.
- NNLO results available at finite T and quark chemical potential(s).
- Result on the right is for a single quark chemical potential.
- Result is completely analytic.
- Residual dependence on the RG scales Λ_g and Λ_q .

$$\begin{aligned}
\frac{\Omega_{\text{NNLO}}}{\Omega_0} = & \frac{7}{4} \frac{d_F}{d_A} \left(1 + \frac{120}{7} \hat{\mu}^2 + \frac{240}{7} \hat{\mu}^4 \right) + \frac{s_F \alpha_s}{\pi} \left[-\frac{5}{8} (1 + 12\hat{\mu}^2) (5 + 12\hat{\mu}^2) + \frac{15}{2} (1 + 12\hat{\mu}^2) \hat{m}_D \right. \\
& + \frac{15}{2} \left(2 \ln \frac{\hat{\Lambda}_q}{2} - 1 - \aleph(z) \right) \hat{m}_D^3 - 90 \hat{m}_q^2 \hat{m}_D \Big] + s_{2F} \left(\frac{\alpha_s}{\pi} \right)^2 \left[\frac{15}{64} \left\{ 35 - 32 (1 - 12\hat{\mu}^2) \frac{\zeta'(-1)}{\zeta(-1)} + 472 \hat{\mu}^2 \right. \right. \\
& + 1328 \hat{\mu}^4 + 64 \left(-36 i \hat{\mu} \aleph(2, z) + 6(1 + 8\hat{\mu}^2) \aleph(1, z) + 3i \hat{\mu} (1 + 4\hat{\mu}^2) \aleph(0, z) \right) \Big\} - \frac{45}{2} \hat{m}_D (1 + 12\hat{\mu}^2) \Big] \\
& + \left(\frac{s_F \alpha_s}{\pi} \right)^2 \left[\frac{5}{4\hat{m}_D} (1 + 12\hat{\mu}^2)^2 + 30 (1 + 12\hat{\mu}^2) \frac{\hat{m}_q^2}{\hat{m}_D} + \frac{25}{12} \left\{ \left(1 + \frac{72}{5} \hat{\mu}^2 + \frac{144}{5} \hat{\mu}^4 \right) \ln \frac{\hat{\Lambda}_q}{2} \right. \right. \\
& + \frac{1}{20} (1 + 168\hat{\mu}^2 + 2064\hat{\mu}^4) + \frac{3}{5} (1 + 12\hat{\mu}^2)^2 \gamma_E - \frac{8}{5} (1 + 12\hat{\mu}^2) \frac{\zeta'(-1)}{\zeta(-1)} - \frac{34}{25} \frac{\zeta'(-3)}{\zeta(-3)} \\
& - \frac{72}{5} [8\aleph(3, z) + 3\aleph(3, 2z) - 12\hat{\mu}^2 \aleph(1, 2z) + 12i \hat{\mu} (\aleph(2, z) + \aleph(2, 2z)) - i \hat{\mu} (1 + 12\hat{\mu}^2) \aleph(0, z) \\
& \left. \left. - 2(1 + 8\hat{\mu}^2) \aleph(1, z) \right\} - \frac{15}{2} (1 + 12\hat{\mu}^2) \left(2 \ln \frac{\hat{\Lambda}_q}{2} - 1 - \aleph(z) \right) \hat{m}_D \right] \\
& + \left(\frac{c_A \alpha_s}{3\pi} \right) \left(\frac{s_F \alpha_s}{\pi} \right) \left[\frac{15}{2\hat{m}_D} (1 + 12\hat{\mu}^2) - \frac{235}{16} \left\{ \left(1 + \frac{792}{47} \hat{\mu}^2 + \frac{1584}{47} \hat{\mu}^4 \right) \ln \frac{\hat{\Lambda}_q}{2} - \frac{144}{47} (1 + 12\hat{\mu}^2) \ln \hat{m}_D \right. \right. \\
& + \frac{319}{940} \left(1 + \frac{2040}{319} \hat{\mu}^2 + \frac{38640}{319} \hat{\mu}^4 \right) - \frac{24\gamma_E}{47} (1 + 12\hat{\mu}^2) - \frac{44}{47} \left(1 + \frac{156}{11} \hat{\mu}^2 \right) \frac{\zeta'(-1)}{\zeta(-1)} - \frac{268}{235} \frac{\zeta'(-3)}{\zeta(-3)} \\
& \left. \left. - \frac{72}{47} [4i \hat{\mu} \aleph(0, z) + (5 - 92\hat{\mu}^2) \aleph(1, z) + 144i \hat{\mu} \aleph(2, z) + 52\aleph(3, z)] \right\} + 90 \frac{\hat{m}_q^2}{\hat{m}_D} + \frac{315}{4} \left\{ \left(1 + \frac{132}{7} \hat{\mu}^2 \right) \ln \frac{\hat{\Lambda}_q}{2} \right. \right. \\
& \left. \left. + \frac{11}{7} (1 + 12\hat{\mu}^2) \gamma_E + \frac{9}{14} \left(1 + \frac{132}{9} \hat{\mu}^2 \right) + \frac{2}{7} \aleph(z) \right\} \hat{m}_D \right] + \frac{\Omega_{\text{NNLO}}^{\text{YM}}(\Lambda_g)}{\Omega_0}. \quad (5)
\end{aligned}$$

Andersen, Leganger, Su, and MS 1009.4644, 1103.2528
Haque, Andersen, Mustafa, MS, N. Su, 1309.3968

Pressure vs temperature



HTLpt = Andersen, Leganger, MS, and Su 1009.4644, 1103.2528

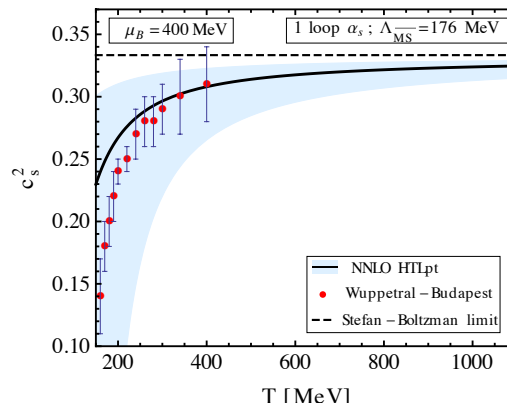
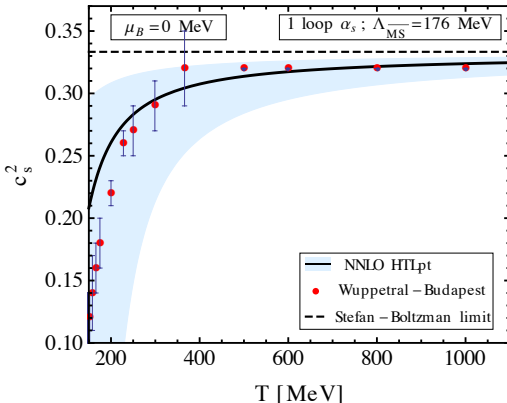
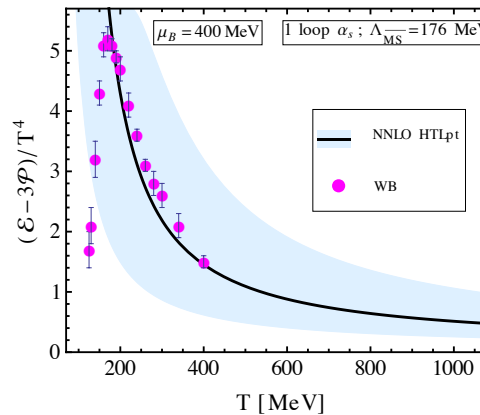
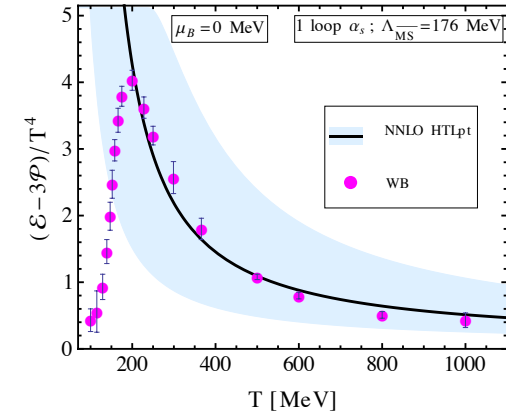
Haque, Andersen, Mustafa, MS, and Su, 1309.3968

EQCD = Ghiglieri, Kurkela, MS, and Vuorinen, 2002.10188

WB = Wuppertal-Budapest lattice calculation

Trace Anomaly and Speed of Sound

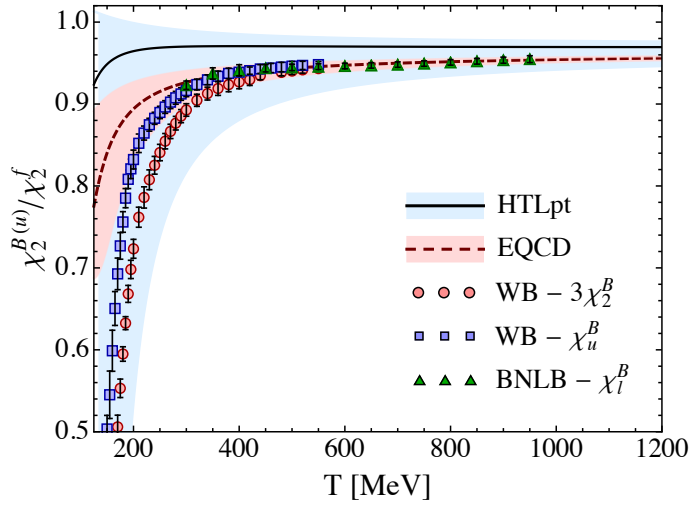
N. Haque, A. Bandyopadhyay, J.O. Andersen, M.G. Mustafa, MS, N. Su, 1402.6907



Quark and baryon number susceptibilities

HTLpt = Haque, Andersen, Mustafa, MS, and Su, 1309.3968

EQCD = Ghiglieri, Kurkela, MS, and Vuorinen, 2002.10188



General Quark Susceptibility

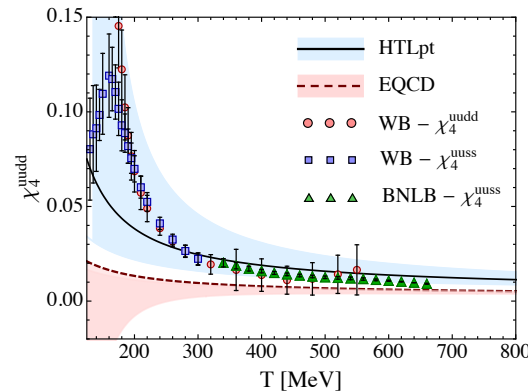
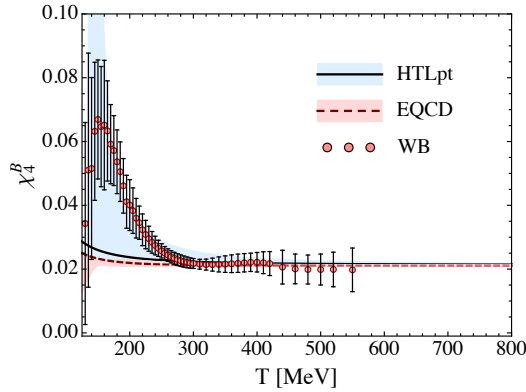
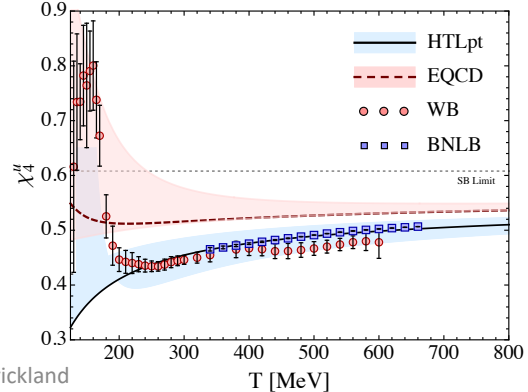
$$\chi_{ijk\dots}(T) \equiv \left. \frac{\partial^{i+j+k+\dots} \mathcal{P}(T, \mu)}{\partial \mu_u^i \partial \mu_d^j \partial \mu_s^k \dots} \right|_{\mu=0}$$

Baryon Number Susceptibility

$$\chi_B^n(T) \equiv \left. \frac{\partial^n \mathcal{P}}{\partial \mu_B^n} \right|_{\mu_B=0}$$

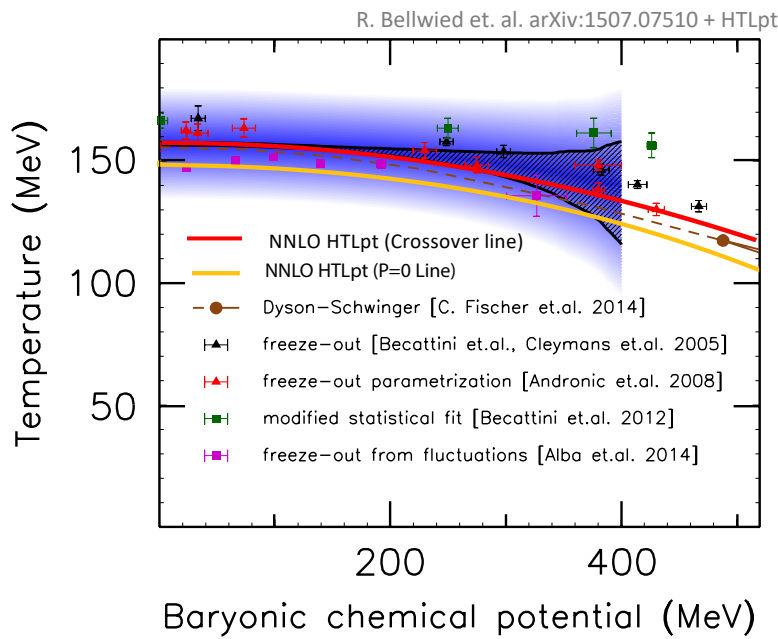
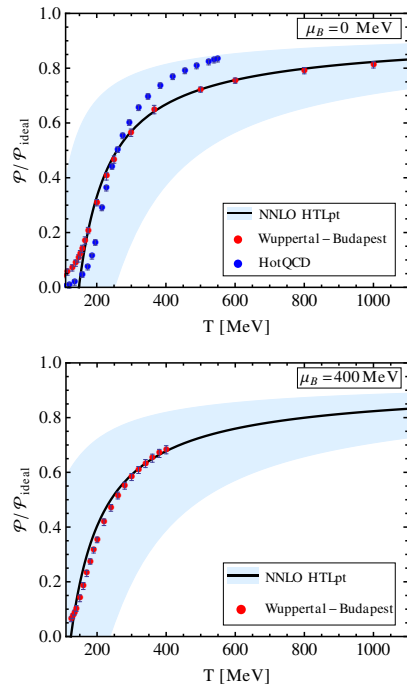
For example

$$\chi_2^B = \frac{1}{9} [\chi_2^{uu} + \chi_2^{dd} + \chi_2^{ss} + 2\chi_2^{ud} + 2\chi_2^{ds} + 2\chi_2^{us}]$$



HTLpt phase transition line

We can solve for the point where the HTLpt pressure goes to zero OR when it drops below the hadron gas pressure in order to extract a phase transition line.

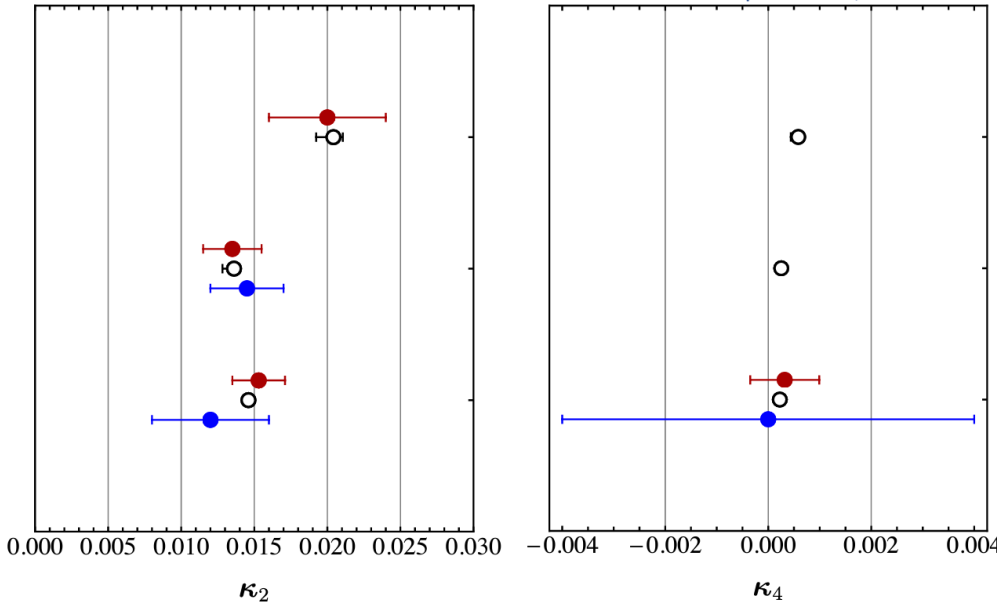


Can extract curvatures defined via the following Taylor series near $\mu=0$

$$\frac{T_c^\mu}{T_c^0} = 1 - \kappa_2 \left(\frac{\mu_B}{T_c^\mu} \right)^2 - \kappa_4 \left(\frac{\mu_B}{T_c^\mu} \right)^4 - \kappa_6 \left(\frac{\mu_B}{T_c^\mu} \right)^6 - \dots$$

Curvature of the phase transition line

Haque and MS, 2011.06938



$$\mu_s = \mu_l = \mu_B/3$$

$$\mu_s = 0, \mu_l = \mu_B/3$$

$$S = 0, Q/B = 0.4, \mu_l = \mu_B/3$$

Lattice data references

- The rows from top to bottom show different physics cases.
- Open circles = HTLpt predictions, closed = lattice results.
- Uncertainties reported for the HTLpt results come from RG scale variation.

- P. Cea, L. Cosmai, and A. Papa, Phys. Rev. D93, 014507 (2016).
- C. Bonati, M. D'Elia, M. Mariti, M. Mesiti, F. Negro, and F. Sanfilippo, Phys. Rev. D92, 054503 (2015).
- C. Bonati, M. D'Elia, F. Negro, F. Sanfilippo, and K. Zambello, Phys. Rev. D98, 054510 (2018).
- S. Borsanyi, Z. Fodor, J. N. Guenther, R. Kara, S. D. Katz, P. Parotto, A. Pasztor, C. Ratti, and K. K. Szabo, Phys. Rev. Lett. 125, 052001 (2020).
- C. Bonati, M. D'Elia, M. Mariti, M. Mesiti, F. Negro, and F. Sanfilippo, Phys. Rev. D90, 114025 (2014).
- A. Bazavov et al. (HotQCD), Phys. Lett. B 795, 15 (2019).

Conclusions

- HTLpt reorganizes the finite temperature expansion of QCD thermodynamics around the classical minimum of the high-temperature effective action.
- In doing so, it improves the convergence of naïve perturbation theory.
- The final NNLO result is completely analytic and valid for all N_c and N_f .
- Comparisons of NNLO HTLpt predictions with lattice data show excellent agreement down to $T \sim 250$ MeV.
- One can also extract the curvature of the phase transition line in three different physical scenarios, again finding excellent agreement with lattice data.
- Renormalization scale dependence is very small yielding precise predictions.